We A3 01

A Robust Multistage Full Waveform Inversion and Its Application

J. Mao* (TGS), J. Sheng (TGS), M. Hart (TGS), T. Kim (TGS)

Summary

High-resolution velocity model building is crucial for depth migration. Inaccurate model will lead to poor image qualities. Full waveform inversion (FWI) is developed to generate more geologically realistic and higher resolution velocity model iteratively. However, it's challenging to apply FWI on narrow azimuth acquisition (NAZ) data. Here we proposed a more robust multistage FWI workflow. For the first stage, we introduce dynamic warping preconditioned full waveform inversion (DWFWI) to mitigate the cycle-skipping problem, which creates large scale background updates. In the second stage, the conventional FWI with image-guided regularization (IGFWI) is introduced to overcome the footprint problem and help the convergence, which can add more detailed updates to the velocity model with much higher resolution with more reflection events included and inverted. Due to poor crossline sampling, FWI updates in the crossline direction always contain strong acquisition footprints and swing artifacts. Image guided regularization is powerful to remove the acquisition footprints as well as preserve the detailed update around the faults. This new workflow is applied on the Hoop Fault Complex data in the southwestern Barents Sea. A more geologically realistic and higher-resolution model of the Hoop Fault Complex is obtained with improved migration image and gathers significantly.

Introduction

High-resolution velocity model building is a very important step in depth imaging. Without an accurate model, it may introduce a lot of artifacts or distortions in migration image. Full waveform inversion (FWI) (Pratt et al., 1998; Virieux and Operto, 2009) has been proposed to achieve a higher resolution velocity update which follows the geological structures. FWI is an inversion method based on minimizing the differences between field recorded and synthetic seismic data. When the time shifts between the synthetic and observed data are too large (more than one half cycle), FWI cannot converge as it will fall into the local minimum. To mitigate the cycle skipping problem, a good starting model is needed such as a previous reflection tomography model. We can also use multiscale inversion starting from a low frequency and gradually increasing to a higher frequency, or choose other objective functions, which may be less affected by cycle-skipping.

Here, we propose a multistage FWI workflow which is more robust for real data application. Dynamic warping preconditioned FWI (DWFWI) preconditions the observed data through dynamic warping such that the preconditioned data is within one half period shift from the synthetic data. DWFWI can provide a closer model with large scale background updates. After DWFWI, the conventional L2-norm FWI with image guided regularization (IGFWI) is performed to get a higher-resolution model update. For NAZ acquisition, poor crossline sampling can cause strong acquisition footprints in the FWI update even after we apply preconditioning to the FWI gradient with illumination compensation (diagonal Hessian). These footprints can be reduced by some regular smoothing operator or K-domain filter. However, some detailed updates can also be destroyed by these operations. Image guided regularization can be utilized to further reduce the footprint effects while we preserve the sharp contrast update around the some key structures (e.g. faults).

This multistage FWI workflow (DWFWI + IGFWI) is applied to a NAZ data set, the Hoop Fault Complex, which is 2770 km^2 acquired in 2009, located in the region of the Norwegian Barents Sea, and divides the Loppa High and Bjameland Platform. If the velocity model is not built correctly across the fault boundary, a typical fault shadow imaging problem will occur and big distortions in the depth of the structure can be introduced. Large fault sags will show up within the footwall of the major trending extensional fault in the survey area, as well as numerous smaller distortions associated with complex faulting within the high velocity Lower Cretaceous overburden. There are several prior attempts to solve the fault shadow problem. Rodriguez et al. (2011) used surface-constrained tomography in this area, where velocity models were separated by an interpreted fault and updated independently. Hart et al. (2015) used offset-dependent picking and image-guided tomography (IGT) for a higher resolution and more geologically consistent approach to tomographic model building. Here we are trying to further improve the model resolution and accuracy with FWI. We use the IGT velocity model as the initial model for FWI. We first apply DWFWI to solve the major traveltime difference of the early refraction arrivals and get a model without cycle-skipping. Then the IGFWI is employed for a high-resolution update. Image-guided regularization can reduce the footprint effect while preserving the sharp contrast around the faults. A much higher resolution model results from this multistage FWI workflow. After FWI, we also applied an additional tomography to update the deep portion and avoid some overcorrected updates from FWI. The improvement from the advanced model-building approach is verified with the stacked image and common image gathers (CIG).

Multi-stage FWI workflow

The first stage our FWI workflow is the DWFWI. Dynamic warping (DW) (Hale, 2013) is a method to estimate relative time shifts between two dataset. DW works much better than crosscorrelation-based methods when the shifts are large and vary rapidly with time and space. Here we precondition the observed data through DW for refraction FWI. The preconditioned data is the shifted synthetic data through DW. With limited maximum time shift in DW, the warped data is within one half period time shift from the synthetic data for each shot during each iteration, which avoids cycle-skipping. Figure 1 shows the starting model and velocity update with DWFWI (up to 10Hz) for the Hoop Fault Complex data set, which is mainly a low-wavenumber background velocity update. After DWFWI,

we have better matched the early arrival refraction events when we compare the observed data and synthetic data. Figure 2 plots the correlation map (before and after FWI) between observed data and synthetic data. This statistic QC verified our DWFWI did a good job in the entire survey area. We also QC with depth migrated common image gathers which shows better flatness, the DWFWI with refraction traveltime is very robust for the background update.
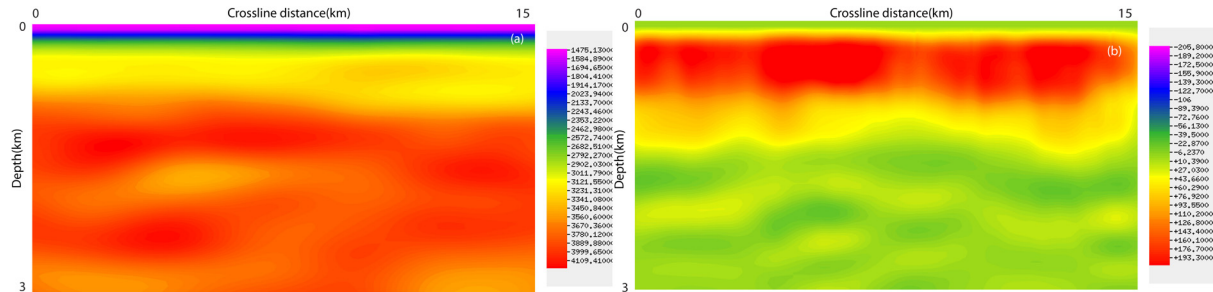

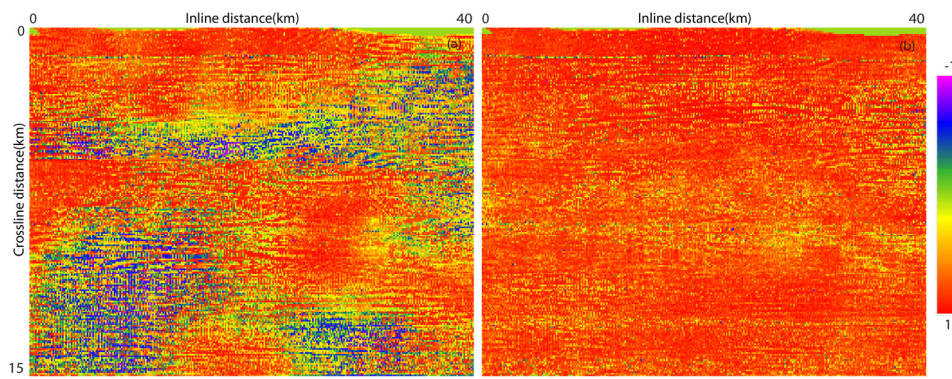**Figure 1** *crossline section: (a) the starting velocity; (b) the velocity update from DWFWI.*

Figure 2 *Correlation map between synthetic and observed data: (a) with the starting velocity; (b) with the velocity update from DWFWI.*
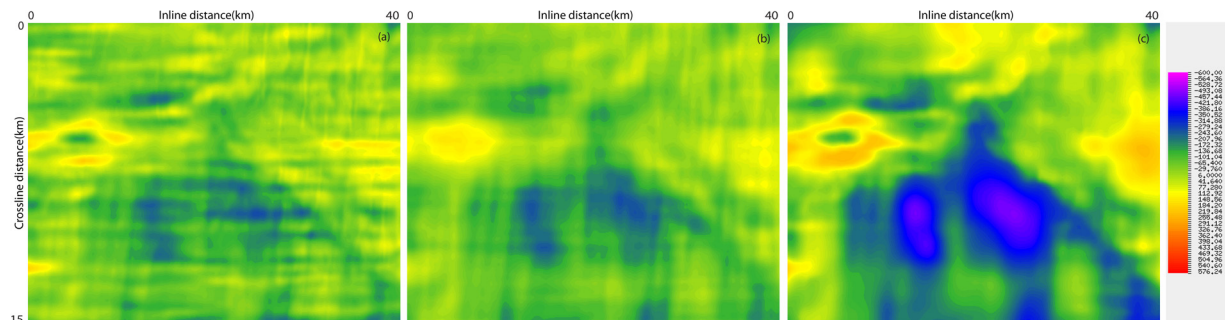

Figure 3 *Comparison of FWI updates at depth 1050m: (a) without preconditioning; (b) with regular smoothing; (c) with IG preconditioning.*

In the second stage, we try to obtain a much higher resolution update through IGFWI. After DWFWI, we mitigate the cycle-skipping problem and get a more accurate starting velocity model. Then we can run the conventional FWI to get further updates in a multiscale way, which means we run FWI to match the data from low frequency to high frequency (up to 15Hz). During the application of FWI on a NAZ data, we noticed a very strong acquisition footprint effect in the FWI update. First, we applied preconditioning to the FWI gradient with illumination (diagonal Hessian) which makes the update much more balanced, but the footprint effect is reduced but still there. Besides the footprint, we also notice swing artifacts on the FWI gradient due to insufficient acquisition coverage in the crossline direction. Therefore we must apply smoothing preconditioning on the FWI gradient to avoid an inaccurate update. The resolution of the update with regular smoothing is decreased a lot while reducing the footprint. This is why we adopted image-guided regularization which is superior to the

regular smoothing method. Figure 3 is the comparison of different preconditioning methods on FWI gradient. We can see a very strong footprint in the crossline direction due to the NAZ acquisition in Figure 3a. With a regular smoothing method, we get a velocity update as Figure 3b shows. Figure 3c shows FWI with IG preconditioning, which is free of the footprint problem and the update is blocky. By comparing Figures 3b and 3c, we note as another important feature that the IGFWI preserved the sharp boundaries of the velocity update along the major faults.
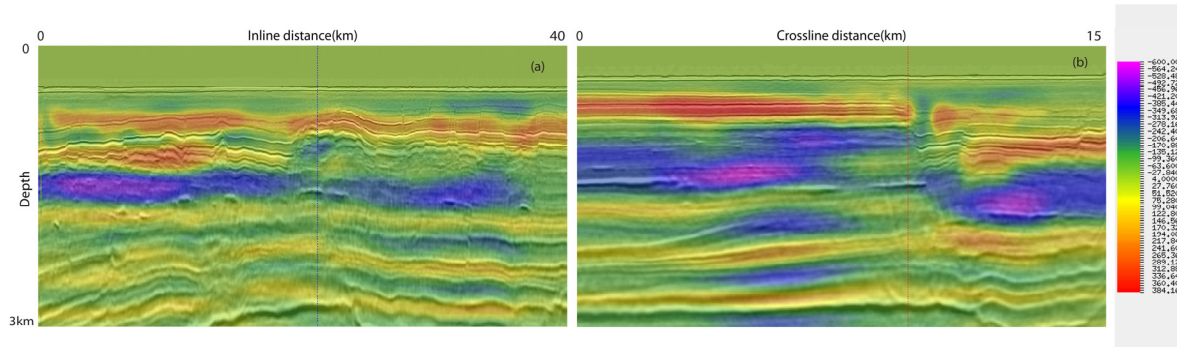
Field data example

Figure 4 *FWI velocity update overlaid on migration stack image: (a) an inline section; (b) a crossline section.*
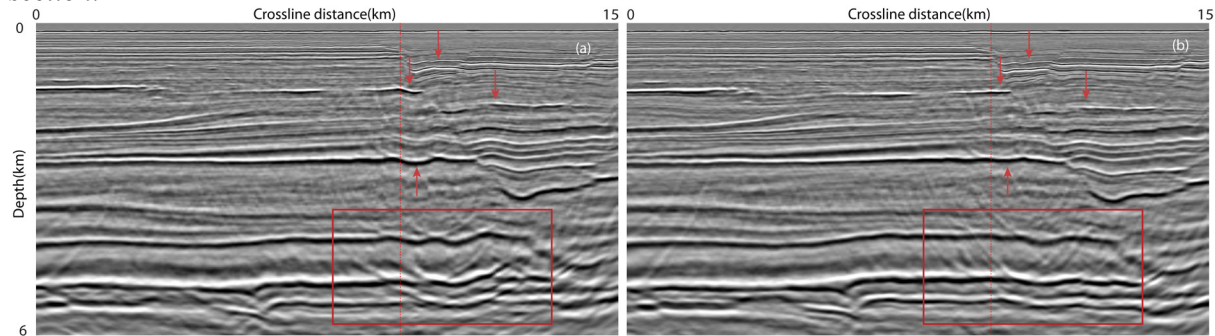

Figure 5 *Depth migration image of a crossline section: (a) migration with the initial model; (b) migration with the updated model.*
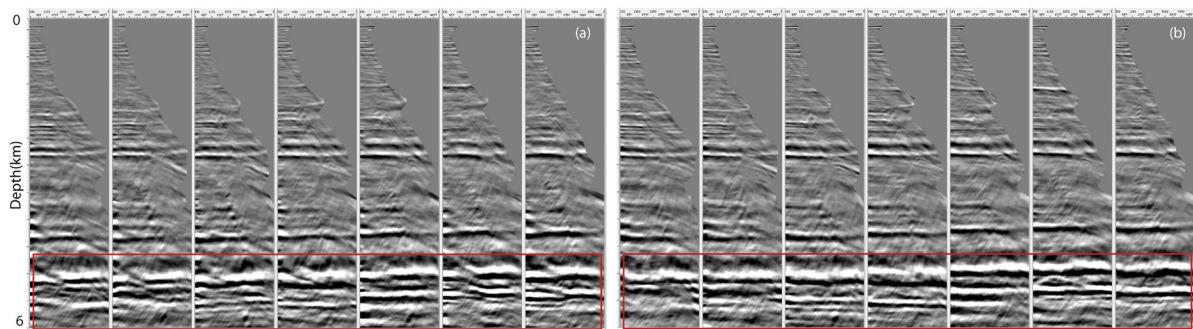

Figure 6 *Common image gathers of a crossline section: (a) CIG with the initial model; (b) CIG with the updated model.*

Our testing area in Hoop Fault Complex is 15 km by 40 km. Shot and receiver intervals are 18.75 m and 12.5 m. The streamer cable length is 6 km. The shot record length is 7.1 seconds. The sea bottom is nearly flat in the depth range of 0.43 km ~ 0.46 km. For the FWI test, the maximum frequency is up to 15 Hz. We applied some minor noise removal to the data set, but deghosting and demultiple were not applied. We begin with a Ricker wavelet for modelling and then get an updated source wavelet for inversion. We use the anisotropic VTI acoustic wave equation with a free-surface boundary condition. Anisotropic parameters ε and δ were fixed and only the vertical velocity was updated. We began the DWFWI with the transmitted early arrivals to update the lowest wavenumber velocity structure. After

the major update is complete, additional iterations of IGFWI were run sequentially with multi-frequency bands on top of the FWI velocity generated at the previous inversion stage. This multistage FWI gradually added high wavenumber structures to the velocity model. Because the main contribution of FWI is refraction energy and the main update is in the shallow part (up to 3 km), we run an additional tomography to update the deep portion and also to avoid few overcorrected updates from FWI.

Figure 4 is the FWI velocity update overlaid on the depth migration image. The negative update stops right at the major faults. Figure 4a and Figure 4b are an inline section and a crossline section of FWI update respectively, which are consistent with the real events. The sharp contrast on the update results from the multistage FWI update. The depth migration image with the initial model is shown in Figure 5a and the image with the updated velocity model is plotted in Figure 5b. From the comparison, we can see the sags are greatly reduced in the fault shadow area, which is more sensible geologically from an interpreter's point of view. The deep events become more continuous and focused. Figure 6 is the extracted common image gathers in this crossline section. Not only is the gather flatness improved, but also the broken gathers heal because of a more accurate model.

Conclusions

We present a robust multistage full waveform inversion methodology for practical high-resolution velocity model building. In the first stage, the newly developed DWFWI provides long-wavelength updates without cycle skipping. Then IGFWI is utilized to get a higher resolution update. IGFWI is introduced to reduce the footprint effects caused by NAZ acquisition and preserve the sharp contrast around the faults. A much higher resolution model update is obtained after this multistage FWI. We also have an additional tomography after FWI is done. Significant improvements can be seen from both the stacked image and common image gathers on the Hoop Fault Complex field data example, which proved the effectiveness of our multistage FWI workflow.

Acknowledgements

References

Hale, D. [2013] Dynamic warping of seismic images, *Geophysics*, **78**(2), S105–S115.

Hart, M., Adewumi O., Lang C., Hilburn G., and Rodriguez G. [2015] High resolution velocity model building over the Hoop Fault Complex, *85th Annual International Meeting, SEG, Expanded Abstracts*, 5189-5193.

Pratt, R. G., Shin C., and Hicks G. J. [1998] Gauss-Newton and full Newton methods in frequency-space seismic waveform inversion, *Geophysical Journal International*, **133**, 341–362.

Rodriguez, G., Lundy A., Hart M., Lang C., Cai J., Chang I. and Zhang Q. [2011] Imaging the Hoop Fault complex via horizon and fault constrained tomography: *81st Annual International meeting, SEG, Expanded Abstracts*, 4025-4029.

Virieux, J., and Operto S., [2009] An overview of full waveform inversion in exploration geophysics, *Geophysics*, **74**(6), WCC1–WCC26.